Evaluating the Gear Stress of Novel Reverse Rotation Bit Manual Screwdriver Design for Miniscrew Implants

Rizki Aldila Umas, Sugeng Supriadi, Yudan Whulanza, Andi Aditya Ahmad Fauzi Hasan*
Department of Mechanical Engineering, Faculty of Engineering, Universitas Indonesia, Kampus UI Depok 16424, Indonesia
**sugeng@eng.ui.ac.id*

Prasetyanugraheni Kreshanti
Cleft and Craniofacial Center Cipto Mangunkusumo Hospital – Plastic and Reconstructive Surgery Division, Department of Surgery, Faculty of Medicine, Universitas Indonesia, Indonesia

ABSTRACT

One of the problems faced by the screwdrivers used for craniomaxillofacial implant fixation is that the maximum torque required for implant removal is significantly higher than the maximum torque needed for inserting implants. Another problem is that the hand torque produced by a right-handed person is lower in the counterclockwise direction, which is the removal direction for miniscrews. The novel design presented here of a manual screwdriver equipped with an epicyclic gear will produce a reverse bit rotation and provide the mechanical advantage of higher torque output. In this study, simulations were conducted by varying the torque input within the range of 0-1000 Nmm with an applied load in each simulation to be adapted based on the epicyclic gear set. The materials used in this study are AISI 316L and Ti6Al4V. The maximum Von Mises stress value was observed in the sun gear from the second gear set at 522.59 MPa (AISI 316L) and 430.76 MPa (Ti6Al4V) for the maximum torque input, which was followed by the planetary and ring gear from the second gear set and then the planetary gear, ring gear, and sun gear from the first gear set. The total deformation also showed the difference between the two materials; the deformation when using AISI 316L as the material was lower than when using Ti6Al4V.

ISSN 1823-5514, eISSN 2550-164X
Received for review: 2020-12-01
Accepted for publication: 2020-12-19
Published: 2021-01-15

Keywords: *Surgical Screwdriver; Epicyclic Gear; Maxillofacial Implant*

Introduction

A screwdriver is the primary tool for the insertion and removal of miniscrew implants, which means that a surgeon's performance is highly dependent on them. One widely used screwdriver handle for miniscrew implants consists of two parts: the front and rear. The front part is rotatable and is usually rotated by the user's fingers (Figure 1), while the rear part fits into the palm of the user's hand, which is held fixed [1]. Some studies have reported making improvements in miniscrew surgical screwdrivers that include the ability to limit torque in miniscrew insertion in order to avoid a stripping of the bone caused by over torque [2] and a modification that adds an auxiliary positioning attachment in order to achieve a precise height for avoiding any tissue injuries [3].

However, the screwdriver design that is now widely used could be improved for even better performance to support surgeons. For example, there are some problems related to the osseointegration of the miniscrew and the hand's natural movement. One such problem is the higher torque needed for removing miniscrew implants. As widely used, reliable implants that provide temporary anchorage for orthodontics and craniomaxillofacial treatments [4], [5], miniscrew implants are usually made from titanium [5], [6], and in some cases need to removed once the treatment is finished (for temporary anchorage) or due to problems that occur after miniscrew implant placement. Even though there are biodegradable mini-implants, including miniscrews, due to their high pricing they are not much used in surgery [7]. A titanium miniscrew is manufactured as an untreated, smooth surface that will result in osseointegration or partial osseointegration. Studies [6], [8] show that the maximum removal torque of the miniscrews is significantly higher than the maximum insertion torque because of the osseointegration or partial integration of the miniscre.

Another problem that needs to be solved is the lower torque generated by the human hand due to the miniscrew removal motion and the screwdriver's geometry. The maximum torque produced by a right-handed person is lower in the counterclockwise direction [9], [10], which happens to be the motion for the removal of a miniscrew (Figure 1). Moreover, the maximum torque produced in two studies [9], [11] shows that even using the same motion, different torques were measured. One reason for this could be the difference in each circular object diameter. The smaller diameter of the circular object is subjected to a lower maximum torque that can be exceeded by hand [12]. As a medical device for inserting and removing miniscrews, surgical screwdrivers generally have a smaller diameter than the ones studied

(4.5 and 6.6 cm) [9], [11] which could result in a low maximum torque of a surgeon's hand due to their small diameter. Several studies found that the maximum value of torque generated by human fingers during screw insertion motion (clockwise direction) was 420 Nmm [13]–[16].

Figure 1: (a) The initial motion of a miniscrew removal, (b) the maximum counterclockwise motion for the fingers, and (c) returning to the position for the next motion in removing the miniscrew.

One solution for both rotation direction and torque needs is an epicyclic gear. The epicyclic gear could give the reversed bit rotation a mechanical advantage through its configuration. That mechanical advantage is determined by the gear ratio and its relation to torque; a higher gear ratio will produce a more significant output torque for the same input torque. Concerning the epicyclic gear itself, many configurations can produce different results based on its input, output, or stationary components [17], [18], its rotational speed, torque, and direction of the rotation. In this research, we will use two combinations; each of them has a different function but will create a reversed bit rotation and mechanical advantage at the same time. Therefore, the purpose of this study was to evaluate the stress in the epicyclic gear for a new manual screwdriver designed for the removal of miniscrew implants.

Methodology

Model and Design

The present study's screwdriver was designed using SolidWorks®. It has a round-shaped handle, which demonstrated the best ergonomics [2] when

tested by several Indonesian surgeons. In this design, a shaft will hold the ring gear in the second epicyclic gear set; it will automatically define the upper side of the screw because the shaft is immovable. There is no study yet about determining the size of the shaft that will not disturb the ergonomics of the screwdriver that could affect a surgeon's performance. The full design of the screwdriver is shown in Figure 2.

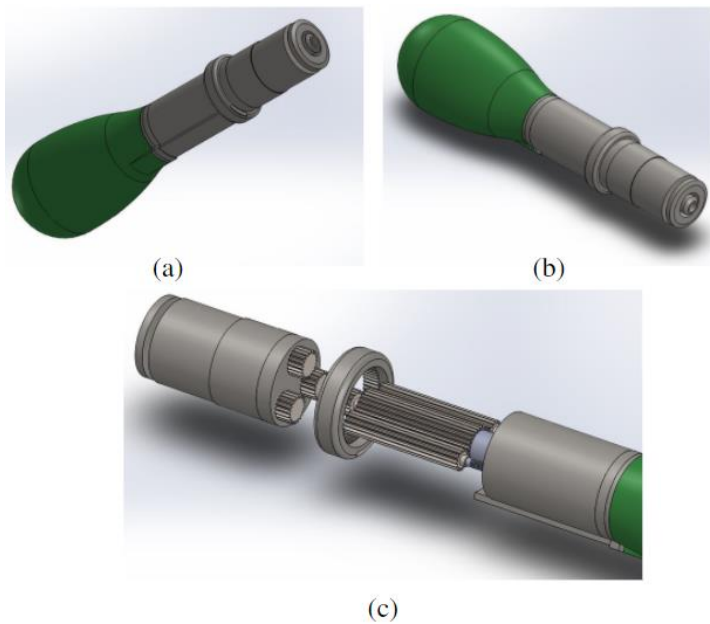

Figure 2: (a,b) overall screwdriver design and (c) epicyclic gear sets.

In this design, two sets of epicyclic gears are used, one for reversing the rotation of the bit and the other for gaining a mechanical advantage. The main reason the screwdriver needs two sets of epicyclic gears is because the first gear set (that reverses the rotation of the bit) will give this system lower torque output (based on the gear ratio, it will be lower than 1), which is not desirable in this design. Therefore, the second gear set is needed to give the mechanical advantage of higher torque output, which counteracts the undesirable effect of the first set. The arrangement of the epicyclic gears is shown in Figure 3. In the first epicyclic gear set, the planetary carrier (in this case, the handle of the screwdriver) is held stationary, so that the input of this system is in the ring gear and the output is in the sun gear. The first epicyclic gear set's sun gear is connected to the sun gear of the second epicyclic gear set, and, by holding the ring gear in this set (second gear set) stationary, the

planetary gear will rotate on its axis and revolve around the sun gear. That movement will cause the planetary carrier to become the output, transmitting the torque generated to the screwdriver's bit. The specifications of those two sets of epicyclic gears (all of them using the modified ISO standard in SolidWorks®) are shown in Table 1.

Table 1: Epicyclic gear set specification

Parts	Quantity	Module (mm)	Teeth	Pressure Angle (°)	Face Width (mm)
First Gear Set					
Sun Gear	1	0.25	28	20	24
Planetary Gear	2	0.25	15	20	24
Ring Gear	1	0.25	58	20	24
Second Gear Set					
Sun Gear	1	0.25	18	20	3
Planetary Gear	3	0.25	20	20	3
Ring Gear	1	0.25	58	20	3

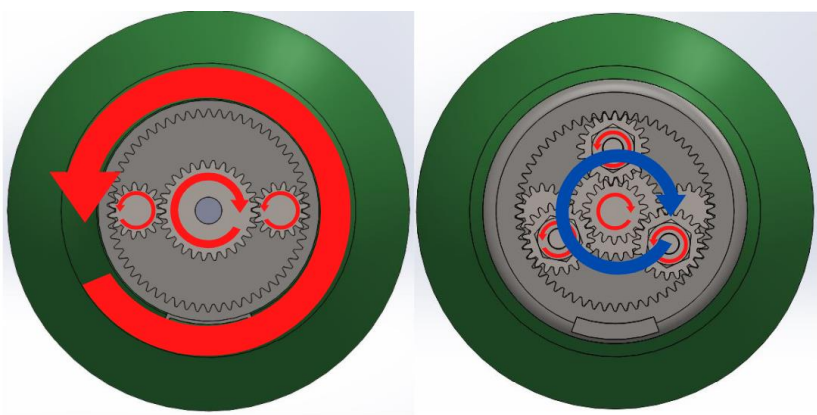

Figure 3: (a) First gear set's and (b) second gear set's movements. Both sun gears are designed to be in one shaft (see Figure 2).

The above specifications (Table 1) will create a mechanical advantage, which is one of the main developments of this screwdriver. The mechanical advantage from the epicyclic gear sets can be calculated using Equation (1),

with the number showing the position of each gear set and the letters representing the names of the components (S and R refer to the sun and ring gears):

$$\text{Gear Ratio} = \frac{\text{Torque Out}}{\text{Torque In}} = \left(\frac{N_{S1}}{N_{R1}}\right) \times \left(1 + \frac{N_{R2}}{N_{S2}}\right) \quad (1)$$

In Equation (1), we can find that the first half of the equation (the first gear set's R1 and S1) will produce a value less than one, which is the undesirable effect of the first gear set (the reverse function) arising from its lower output torque. The other half of the equation is the gear ratio of the second gear set, the higher gear ratio value of which can remove the undesirable effect of the first gear set and, according to the equation, will produce an output torque double the value of the input torque. This epicyclic gear arrangement will solve the need for higher torque in miniscrew removals by adding a mechanical advantage that will produce a torque output about twice the insertion torque.

Finite Element Analysis

This novel design was tested by simulation software (ANSYS®) to determine the stress distribution for each component. The main focus of this design test is the torque load inserted in the input ring gear (the ring gear in the first gear set) while holding the output (the carrier of the planetary gear in the second gear set) stationary. This will simulate the real-world conditions in which the screwdriver is used with a miniscrew strong enough to hold the load applied. These operating conditions were chosen for the simulation according to ISO 6336-1, which states that the most reliable known approach to the appraisal of overall system performance is testing a proposed new design [19].

In this simulation, AISI 316L and Ti6Al4V were used for the material. Both materials were chosen because they are widely used in biomedical applications, especially for surgical instruments, and because they are biocompatible. Both materials are considered light compared to the carbon steels commonly used in epicyclic gear [20], and both possess considerably high strength, which becomes crucial related to biomedical application designs in which a low failure rate is a primary consideration [21]. The mechanical properties of the material used are listed in Table 2.

Table 2: Mechanical properties of the material used in the simulation in SI

Properties	AISI 316 L	Ti6Al4V
Young Modulus (GPa)	193	119
Poisson's Ratio	0.25	0.37
Density	8000	4512
Ultimate Tensile Strength (MPa)	515	1200
Yield Strength (MPa)	205	862

The geometry for this simulation is simplified to shorten the simulation time needed to resolve this problem. The simplification pays attention to the minimum parts used for testing how they affect the results of the gear stress simulation. The torque in this simulation was designed to be varied from 0 to 1000 Nmm; this value was used considering that the removal torque value in several studies did not exceed 1000 Nmm [6], [22]. A perfect planetary gear (with no errors) will carry the same load in each planetary gear; however, manufacturing and assembly errors could create differences in each gear load [23]. Therefore, the simplification of the geometry used here will determine one of the planetary gears for each gear set with the load adjusted to the proportion between load and the number of planetary gear. For instance, the first planetary gear load is adjusted to up to 500 Nmm (ring gear) because we only use one planetary gear instead of two. The load for the second gear set must then be set up to at least 161 Nmm since the output torque from the first gear set is divided by 3 (160.9 Nmm).

Hex-dominant is used for model meshing [24], with refinement in specific areas defined as the contact area. Some bearings are involved in the design and will be represented by revolute joints. Two finite element analyses will be conducted for analyzing each gear. For the first gear set, the analysis was conducting by adding joint load (0-500 Nmm) in the ring gear and fixing the support in the sun gear (Figure 4). In this analysis, the model was meshed by 1,378,584 nodes and 930,563 elements (Figure 5), with the element in the gear tooth that will be in contact having a finer mesh than the whole structure to improve the accuracy of the simulation and to optimize the solving time by having a bigger mesh in the less affected areas. In the second gear set, the analysis was conducted by adding joint moment (0-161 Nmm) in the sun gear and fixing the support in the ring gear (Figure 6); fixed support in the ring gear was added to simulate the shaft that holds the second epicyclic ring gear, steadying it so that the planetary gear carrier could be the output. This analysis model was meshed by 332,831 nodes and 222,914 elements (Figure 7).

Figure 4: Parameters used in the first gear sets with A as fixed support and B as the area where the joint load is applied.

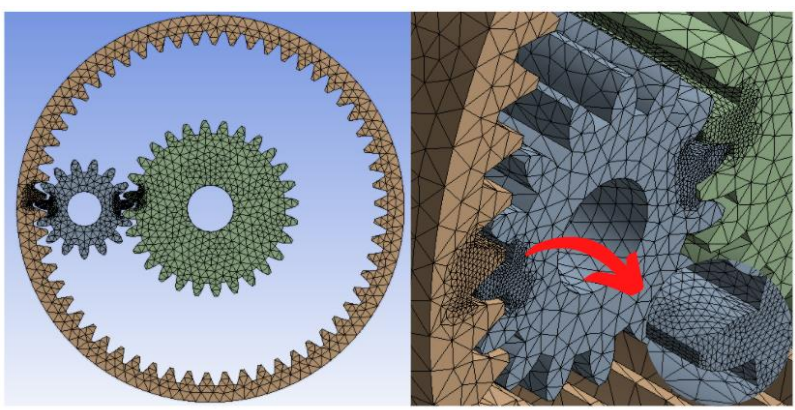

Figure 5: (a) First gear set meshed and (b) refinement in the contact area.

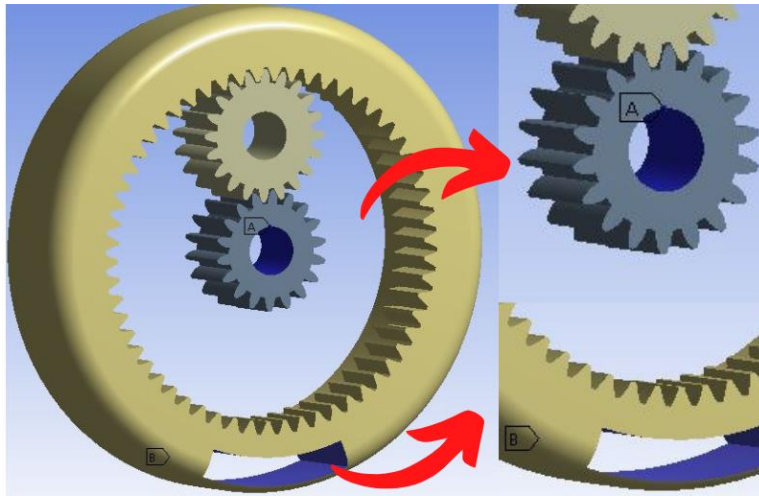

Figure 6: Parameters used in the second gear set with A being the joint load applied area and B as a fixed support.

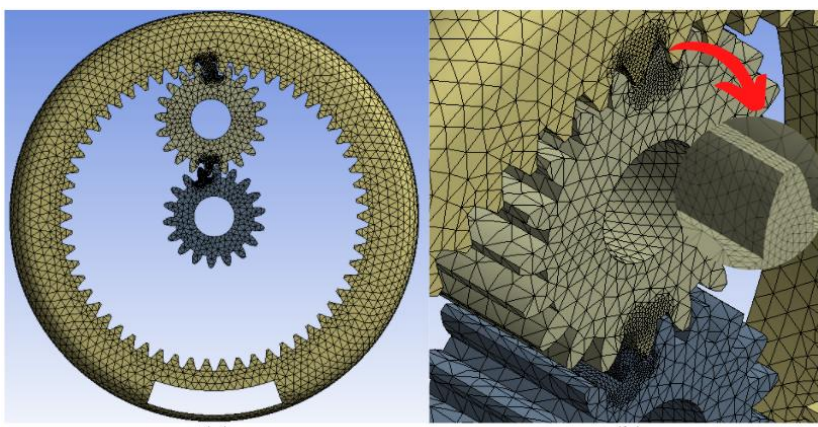

Figure 7: (a) The second gear set meshed and (b) refinement in its contact area.

Results and Discussion

The simulation results are shown in Tables 3 until Table 10; these tables list the maximum Von Mises stress values and total deformation of each part in each gear set. In this study, the overall torque load was designed to increase from 0-1000 Nmm at 200 Nmm increments, but this was adapted for each simulation setting. In other words, each load torque value represented two times its value for the first epicyclic gear sets and three times its value for the second epicyclic gear sets. (As results of the gear ratio of the first gear sets, the value transmitted would not be the same with the input load.) The results for the simulation model that used AISI 316L for its material in Tables 3 and 4 show the maximum Von Misses stress values for each component in each epicyclic gear set, while Tables 7 and 8 show the maximum total deformation in each epicyclic gear set. The maximum Von Mises stress value results for the model using Ti6Al4V are shown in Tables 5 and 6, while Tables 9 and 10 list the total deformation for each component in each epicyclic gear set.

The maximum Von Mises stress values increases linearly, subject to the increment of the load applied. In all of the simulations using different materials and gear sets, the highest maximum Von Misses stress happened in the second gear set with the sun gear, which comes in contact with the second planetary gears that transfer the load to be the screwdriver's output; here, the maximum Von Mises stress in AISI 316 L is higher than in Ti6Al4V. Since the yield strength of AISI 316 L is 205 MPa, it tends to be exceeded by the stress in the second gear set after the second load increment, which was 64.4 Nmm in the simulation with the second gear set (due to the adjustment mentioned before) or equal to 400 Nmm input torque if using designed geometry that has three planetary gears (see Figure 3).

Table 3: Maximum Von Mises stress values in the first epicyclic gear set using AISI 316L for the material

Torque (Nmm)	Maximum Von Mises Stress Value (MPa) (AISI 316L)		
	First Ring Gear	First Planetary Gears	First Sun Gear
500	65.946	103.71	53.741
400	52.768	86.63	45.095
300	39.513	69.394	36.342
200	26.293	52.025	27.453
100	13.162	31.363	14.975

Table 4: Maximum Von Mises stress values in second epicyclic gear set using AISI 316L for material

Torque (Nmm)	Maximum Von Mises Stress Value (MPa) (AISI 316L)		
	Second Ring Gear	Second Planetary Gears	Second Sun Gear
161	345.18	526.90	522.59
128.8	284.64	440.17	452.21
96.6	217.36	341.99	354.30
64.4	146.54	236.53	242.30
32.2	71.279	144.31	139.61

Table 5: Maximum Von Mises stress values in the first epicyclic gear set using Ti6Al4V for the material

Torque (Nmm)	Maximum Von Mises Stress Value (MPa) (Ti6Al4V)		
	First Ring Gear	First Planetary Gears	First Sun Gear
500	64.589	93.778	53.211
400	51.484	79.719	42.889
300	38.654	62.662	32.569
200	25.701	45.431	23.688
100	12.847	27.533	14.132

Table 6: Maximum Von Mises stress values in the second epicyclic gear set using Ti6Al4V for the material

Torque (Nmm)	Maximum Von Mises Stress Value (MPa) (Ti6Al4V)		
	Second Ring Gear	Second Planetary Gears	Second Sun Gear
161	291.53	415.46	430.76
128.8	246.07	372.81	362.36
96.6	201.75	310.75	292.74
64.4	139.11	221.33	217.95
32.2	70.143	124.55	116.65

Table 7: Maximum total deformation in the first epicyclic gear set using AISI 316L for the material

Torque (Nmm)	Maximum Total Deformation (mm) (AISI 316L)		
	First Ring Gear	First Planetary Gears	First Sun Gear
500	8.3481E-03	8.9776E-04	1.5404E-04
400	6.6852E-03	7.2361E-04	1.2295E-04
300	5.7862E-03	5.4773E-04	9.2204E-05
200	3.3409E-03	3.7140E-04	6.1868E-05
100	1.6749E-03	1.9125E-04	3,1188E-05

Table 8: Maximum total deformation in the second epicyclic gear set using AISI 316L for the material

Torque (Nmm)	Maximum Total Deformation (mm) (AISI 316L)		
	Second Ring Gear	Second Planetary Gears	Second Sun Gear
161	2.6871E-02	3.3386E-02	3.5439E-02
128.8	2.1571E-02	2.6859E-02	2.8552E-02
96.6	1.6231E-02	2.0261E-02	2.1580E-02
64.4	1.0863E-02	1.3617E-02	1.4547E-02
32,2	5.4467E-03	6.8665E-03	7.3664E-03

Table 9: Maximum total deformation in the first epicyclic gear set using Ti6Al4V for the material

Torque (Nmm)	Maximum Total Deformation (mm) (Ti6Al4V)		
	First Ring Gear	First Planetary Gears	First Sun Gear
500	1.2573E-02	1.3959E-03	2.5601E-04
400	1.0041E-02	1.1225E-03	2.0439E-04
300	7.5418E-03	8.5012E-04	1.5260E-04
200	5.0248E-03	5.7377E-04	1.0089E-04
100	2.5190E-03	2.9611E-04	5.0692E-05

Table 10: Maximum total deformation in the first epicyclic gear set using Ti6Al4V for the material

Torque (Nmm)	Maximum Total Deformation (mm) (Ti6Al4V)		
	Second Ring Gear	Second Planetary Gears	Second Sun Gear
161	4.2601E-02	5.2517E-02	5.5530E-02
128.8	3.4265E-02	4.2328E-02	4.4843E-02
96.6	2.5834E-02	3.2002E-02	3.3972E-02
64.4	1.7313E-02	2.1527E-02	2.2912E-02
32.2	8.7180E-03	1.0919E-02	1.1680E-02

In theory, there are some ways to decrease the maximum stress in the sun gear from the second epicyclic gear set. Increasing the number of planetary gear in this gear set might decrease the maximum Von Mises stress value since the total contact area will increase. Changing the gear tooth size or geometry might also decrease the Von Misses stress value but might also change the gear ratio (which would affect the mechanical advantage of the screwdriver) or increase the handle's size due to an increase of ring gear diameter that could affect the ergonomics of this design.

The stress and deformation distribution for both materials are similar (Figure 8) due to the geometry and condition of the simulations being the same. Both the above pictures were taken when the maximum load occurred and show no difference because the total deformations incurred are small (Tables 7-10). However, each gear component tends to have a large stress concentration in the contact area and the tooth root of the contacted tooth, as shown in Figure 8 and 9. A previous studies shows the same results in terms of stress distribution pattern [25], [26]. The gear tooth's root shows large stress because the contacted gear holds the force transmitted, just like a cantilever, with the root as the fixed base, and the contact area holds the most contact stress between the colliding gear components. Furthermore, the stress concentration also appears near the fixed support area at the ring gear from the second gear set (Figure 10). This demonstrates that the shaft might be objected to a certain amount of movement and requires the right materials and dimensions that would not or would less affect the screwdriver’s ergonomic factors that could affect a surgeon’s performance.

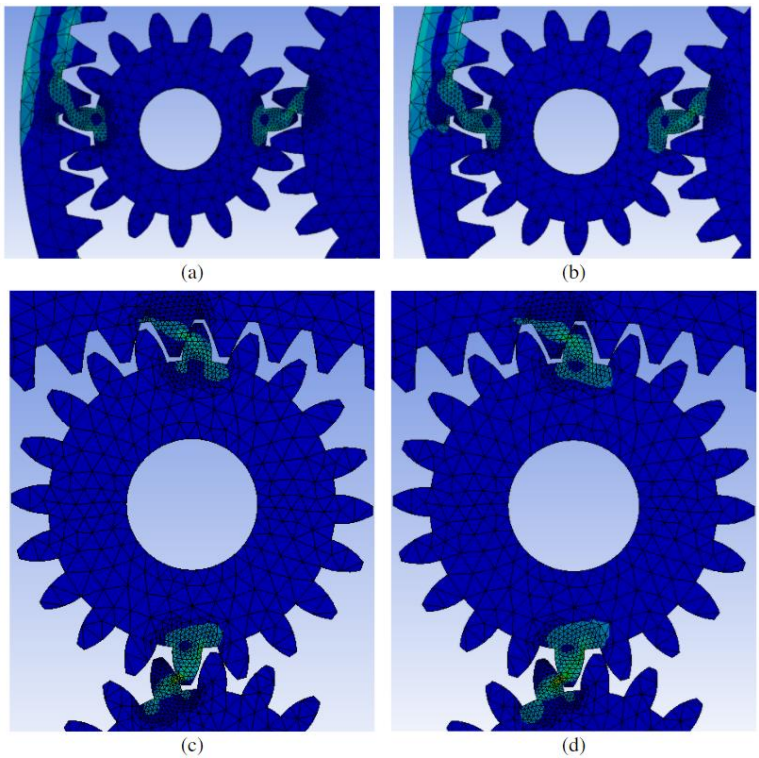

Figure 8: First epicyclic gear set using (a) AISI 316L and (b) Ti6Al4V; and second epicyclic gear set using (c) AISI 316L and (d) Ti6Al4V.

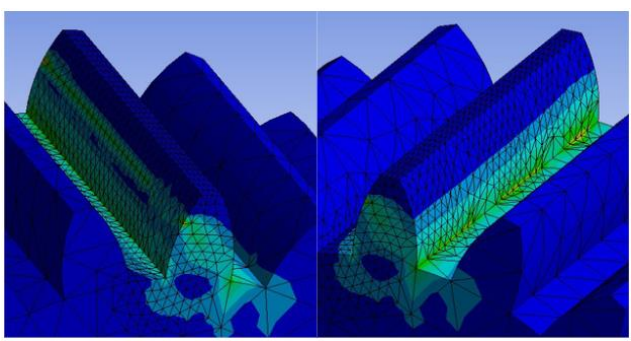

Figure 9: The planetary gear from the second epicyclic gear set shows the stress distribution.

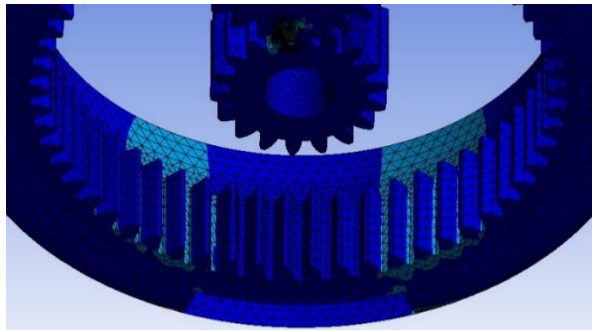

Figure 10: The built-up stress near the fixed support area at the ring gear from the second gear set.

Tables 7 to Table 10 show that the maximum total deformation is related to the stress experienced for each part and the material properties of the model. For instance, the maximum total deformation in the sun gear from the second planetary gear with the highest maximum Von Misses stress value tends to have higher total deformation. The maximum Von Misses stress value is also affected by the material assigned to the model; the maximum total deformation in Ti6Al4V is higher than in AISI 316L, but the maximum Von Misses stress value apparently shows the opposite because AISI 316L has a higher Young's modulus compared to Ti6Al4V, which would make AISI 316L stiffer. The highest maximum total deformation occurs in the sun gear from the second epicyclic gear set when the maximum torque is applied.

Conclusion

A novel design of a manual screwdriver that has reverse rotation and a mechanical advantage was successfully designed. This screwdriver will give about twice the torque in the output compared to the torque input. This simulation-based study shows that the torque input that simulates screwdriver usage will vary in Von Mises stress in each part of the epicyclic gear. In all torque inputs, the highest Von Mises stress always happened in the sun gear from the second epicyclic gear set, followed in order from high to low by the planetary and ring gears from the second gear set and then the planetary, ring, and sun gears from first gear set. The highest Von Misses stress value in each part, as expected, is found at the highest torque input, which represented 1000 Nmm but was adapted in each simulation setting. When AISI 316L was used for the material, the value of each part (from high to low) was 522.59 MPa, 526.90 MPa, 345.18 MPa, 103.71 MPa, 65.946 MPa, and 53.741 MPa.

When Ti6Al4V was used for the material, the value of each part was (from high to low) 430.76 MPa, 415.46 MPa, 291.53 MPa, 93.778 MPa, 64.589 MPa, and 53.221 MPa. The stress values and distribution of each part could be considered for further improvement of this novel design. The simulation's total deformation shows that the deformation that happened when using AISI 316L as the material is smaller than the total deformation when Ti6Al4V was used as the material. This study may need improvement in the screwdriver's design, along with related tests and simulations, to realize the final product.

Acknowledgement

This research work was funded by LPDP Ministry of Finance Republic of Indonesia under Grant Rispro Invitasi 2019 no. UI SK KEP-52/LPDP/2019.

References

[1] K. L. F. Leibinger, "Screwdriver, Particularly for Surgical Purposes," 4.763.548, 1988.
[2] S. Supriadi, R. N. Habibyanto, M. T. Ayman, and W. Muhamad, "Development of screwdriver for maxillofacial miniplate implant with torque-limiting capability," in *AIP Conference Proceedings*, vol. 2092, 2019.
[3] X. Liu, J. Shi, W. Ding, W. Xu, and X. Chen, "The effect of a new modified screwdriver in orthodontic," *Int. J. Clin. Exp. Med.*, vol. 12, no. 8, pp 9706-9711, 2019.
[4] F. D. Uzuner and B. Işık Aslan, "Miniscrew Applications in Orthodontics," in *Current Concepts in Dental Implantology*, 2015.
[5] M. S. M. Pires, L. C. Reinhardt, G. de Marco Antonello, and R. Torres do Couto, "Use of Orthodontic Mini-Implants for Maxillomandibular Fixation in Mandibular Fracture," *Craniomaxillofac. Trauma Reconstr.*, vol. 4, no. 4, pp 213–216, 2011.
[6] E. Y. Suzuki and B. Suzuki, "Placement and removal torque values of orthodontic miniscrew implants," *Am. J. Orthod. Dentofac. Orthop.*, vol. 139, no. 5, pp 669–678, 2011.
[7] S. Fadhilah, A. A. Agus, P. Kreshanti, H. D. S. Budiono, S. Supriadi, and Y. Whulanza, "Engineering economics of cranio-maxillofacial (CMF) degradable implant production in indonesia," in *AIP Conference Proceedings*, vol. 2227, 2020
[8] B. Vande Vannet, M. M. Sabzevar, H. Wehrbein, and K. Asscherickx, "Osseointegration of miniscrews: A histomorphometric evaluation," *Eur. J. Orthod.*, vol. 29, no. 5, pp 437–442, 2007.
[9] J. K. Shim, J. Huang, A. Hooke, M. Latsh, and V. Zatsiorsky, "Multi-

digit maximum voluntary torque production on a circular object," *Ergonomics*, vol. 50, no. 5, pp 660–675, 2007.
[10] J. K. Shim, M. L. Latash, and V. M. Zatsiorsky, "Finger coordination during moment production on a mechanically fixed object," *Exp. Brain Res.*, vol. 157, no. 4, pp 457–467, 2004.
[11] A. I. M. Voorbij and L. P. A. Steenbekkers, "The twisting force of aged consumers when opening a jar," *Appl. Ergon.*, vol. 33, no. 1, pp 105–109, 2002.
[12] Y. K. Kong and B. D. Lowe, "Evaluation of handle diameters and orientations in a maximum torque task," *Int. J. Ind. Ergon.*, vol. 35, no. 12, pp 1073–1084, 2005.
[13] M. Alikhasi, M. Kazemi, H. Jalali, S. Hashemzadeh, H. Dodangeh, and B. Yilmaz, "Clinician-generated torque on abutment screws using different hand screwdrivers," *Journal of Prosthetic Dentistry*, 2017, vol. 118, no. 4, pp 488–492.
[14] F. Parnia, J. Yazdani, P. Fakour, F. Mahboub, and S. M. Vahid Pakdel, "Comparison of the maximum hand-generated torque by professors and postgraduate dental students for tightening the abutment screws of dental implants," *J. Dent. Res. Dent. Clin. Dent. Prospects*, vol. 12, no. 3, pp 190–195, 2018.
[15] Y. Sameera and R. Rai, "Tightening torque of implant abutment using hand drivers against torque wrench and its effect on the internal surface of implant," *J. Indian Prosthodont. Soc.*, vol. 20, no. 2, pp 180, 2020.
[16] A. Kanawati, M. W. Richards, J. J. Becker, and N. E. Monaco, "Measurement of clinicians' ability to hand torque dental implant components.," *J. Oral Implantol.*, vol. 35, no. 4, pp. 185–188, 2009.
[17] I. Hüseyin Filiz, S. Olguner, and E. Evyapan, "A study on optimization of planetary gear trains," in *Acta Physica Polonica A*, 2017, vol. 132, no. 3, pp 728–733.
[18] Q. Zeng, S. Jiang, L. Wan, and X. Li, "Finite element modeling and analysis of planetary gear transmission based on transient meshing properties," *Int. J. Model. Simulation, Sci. Comput.*, vol. 6, no. 3, 2015.
[19] International Standard, *ISO 6336-1: Calculation of Load Capacity of Spur and Helical Gears – Part 1: Basic Principles, Introduction and General Influence Factors. 2nd edition*, 2006.
[20] D. Axinte, Y. Guo, Z. Liao, A. J. Shih, R. M'Saoubi, and N. Sugita, "Machining of biocompatible materials — Recent advances," *CIRP Ann.*, vol. 68, no. 2, pp 629–652, 2019.
[21] H. Delibaş, Ç. Uzay, and N. Geren, "Advanced Material Selection Technique For High Strength and Lightweight Spur Gear Design," *Eur. Mech. Sci.*, vol. 1, no. 4, pp 133–140, 2017.
[22] J. Y. Cha, T. M. Yoon, and C. J. Hwang, "Insertion and removal torques according to orthodontic mini-screw design," *Korean J. Orthod.*, vol. 38,

no. 1, pp 5–12, 2008.
[23] C. G. Cooley and R. G. Parker, "A review of planetary and epicyclic gear dynamics and vibrations research," *Applied Mechanics Reviews*, vol. 66, no. 4, 2014.
[24] Y. Liu, Y. Zhao, M. Liu, and X. Sun, "Parameterized High-Precision Finite Element Modelling Method of 3D Helical Gears with Contact Zone Refinement," *Shock Vib.*, vol. 2019, 2019.
[25] V. Karaveer, A. Mogrekar, T. Preman, and R. Joseph, "Modeling and Finite Element Analysis of Spur Gear," *Int. J. Curr. Eng. Technol.*, 2013.
[26] M. P. Thu and N. L. Min, "Stress Analysis on Spur Gears Using ANSYS Workbench 16.0," *Int. J. Sci. Eng. Appl.*, 2018.